Six new metal-organic frameworks with multi-carboxylic acids and imidazole-based spacer: syntheses, structures and properties

Feng Wang,[‡a] Xiaohuan Ke,[‡a] Jinbo Zhao,[a] Kejian Deng,[b] Xiaoke Leng,[a] Zhengfang Tian,[c] Lili Wen*[a] and Dongfeng Li*[a]

[a] Key Laboratory of Pesticide & Chemical Biology of Ministry of Education, College of Chemistry, Central China Normal University, Wuhan, 430079, P. R. China. Fax: +86 27 67867232; Tel: +86 27 67862900; E-mail: wenlili@mail.ccnu.edu.cn (L. Wen), dfli@ccnu.edu.cn (D. Li)

[b] Key Laboratory of Catalysis and Materials Science of the State Ethnic Affairs Commission & Ministry of Education, South-Central University for Nationalities, Wuhan 430074, P. R. China.

[c] Huanggang Normal Univ, Coll Chem&Appl Chem, Huangguang 438000, P. R. China.

[+]These authors contributed equally to this work.

Table S1 Selected bond lengths (Å) and bond angles (deg) for **1-6**

				1[a]					
Cu1−O1	2.927(2)	Cu1−O2	1.9204(19)	Cu1−N4A	1.9719	Cu1−O1B	2.927(2)	Cu1−O2B	1.9204(19)
Cu1−N4C	1.9719	Cu2−O3	1.9327(19)	Cu2−N1	1.971(2)	Cu2−O5D	2.680(2)	Cu2−O5E	2.680(2)
Cu2−O3F	1.9327(19)	Cu2 −N1F	1.971(2)	O1−Cu1−O1B	180.00	O2−Cu1−O2B	180.00	N4A−Cu1−N4C	180.00
O2B−Cu1−N4C	90.20	O2−Cu1−N4C	89.80	O1B−Cu1−N4A	98.15	O3−Cu2 −O3F	180.00	N1−Cu2−N1F	180.00
O5D−Cu2−O5E	180.00	O3−Cu2−N1	88.76(9)	O3F−Cu2−N1	91.25(9)	O5E−Cu2−N1	87.90(8)		
				2[b]					
Cu1−O1	2.501(2)	Cu1−O2	2.024(2)	Cu1−N1	2.014(3)	Cu1−O1A	2.501(2)	Cu1−O2A	2.024(2)
Cu1−N1A	2.014(3)	O1−Cu1−O1A	134.85(7)	O2−Cu1−O2A	98.66(9)	N1−Cu1−N1A	103.88(12)	O1A−Cu1−O2	93.54(8)
				3[c]					
Zn1−O1	1.947(5)	Zn1−N4	2.006(5)	Zn1−O9B	1.968(5)	Zn1−N8A	2.038(6)	Zn2−O4	1.935(4)
Zn2−O6	1.955(4)	Zn2−N5	2.013(5)	Zn2−N1C	2.035(6)	O1−Zn1−N4	119.5(2)	O1−Zn1−O9B	101.4(2)
O1−Zn1−N8A	101.1(2)	O9B−Zn1−N4	117.4(2)	N4−Zn1−N8A	102.7(2)	O9B−Zn1−N8A	114.1(2)	O4−Zn2−O6	99.68(18)
O4−Zn2−N5	122.7(2)	O4−Zn2−N1C	107.9(2)	O6−Zn2−N5	109.3(2)	O6−Zn2−N1C	114.9(2)	N1C−Zn2−N5	103.0(2)
				4[d]					
Ni1−O1	2.119(2)	Ni1−O5	2.118(2)	Ni1−O7	1.988(2)	Ni1−O1A	2.119(2)	Ni1−O5A	2.118(2)
Ni1−O7A	1.988(2)	Ni2−O1	2.125(2)	Ni2−O1W	2.150(2)	Ni2−O8	2.018(2)	Ni2−N1	2.050(3)
Ni2−O5A	2.101(2)	Ni2−N4A	2.024(3)	O1−Ni1−O1A	180.00	O5−Ni1−O5A	180.00	O7−Ni1−O7A	180.00
O1−Ni1−O5	102.01(8)	O1−Ni1−O7	89.48(8)	O1W−Ni2−O8	168.67(9)	O1−Ni2−N1	167.22(10)	N4A−Ni2−O5A	172.84(10)
				5[e]					
Ni1−O1	2.070(5)	Ni1−O2	2.095(5)	Ni1−O3	2.097(5)	Ni1−N1	2.093(5)	Ni1−N5	2.093(5)
Ni1−N3A	2.108(5)	N1−Ni −N3A	173.3(2)	O1−Ni1−O2	90.79(18)	O3−Ni1−N5	88.76(19)	O2−Ni1−N1	86.47(19)
				6[f]					
Cd1−O1	2.341(2)	Cd1−O9	2.254(4)	Cd1−O1A	2.341(2)	Cd1−O3B	2.396(2)	Cd1−O4B	2.455(2)
Cd1−O3C	2.396(2)	Cd1−O4C	2.455(2)	O1−Cd1−O1A	158.93(8)	O3B−Cd1−O4B	53.87(7)	O3C−Cd1−O4C	53.87(7)
O3C−Cd1−O9	82.88(5)	O4B−Cd1−O9	134.89(5)	O3C−Cd1−O4B	139.86(7)				

[a]Symmetry codes for **1**: (A) -*x*, 1/2+*y*, 3/2-*z*; (B) -*x*, 1-*y*, 3-*z*; (C) *x*, 1/2-*y*, 3/2+*z*; (D) *x*, *y*, 1+*z*; (E) 1-*x*, 1-*y*, 1-*z*; (F) 1-*x*, 1-*y*, 2-*z*

[b]Symmetry codes for **2**: (A) *x*, 3/2-*y*, 1/2-*z*

[c]Symmetry codes for **3**: (A) 3/2-*x*, -1/2+*y*, 1-*z*; (B)3/2+*x*, 1/2-*y*, -*z*; (C)3-*x*, 1-*y*, -1+*z*

[d]Symmetry codes for **4**: (A) 2-*x*, -*y*, 1-*z*

[e]Symmetry codes for **5**: (A) -1+*x*, -1+*y*, *z*

[f]Symmetry codes for **6**: (A) -*x*, *y*, -1/2-*z*; (B) -*x*, -*y*, -*z*; (c) *x*, -*y*, -1/2+*z*.

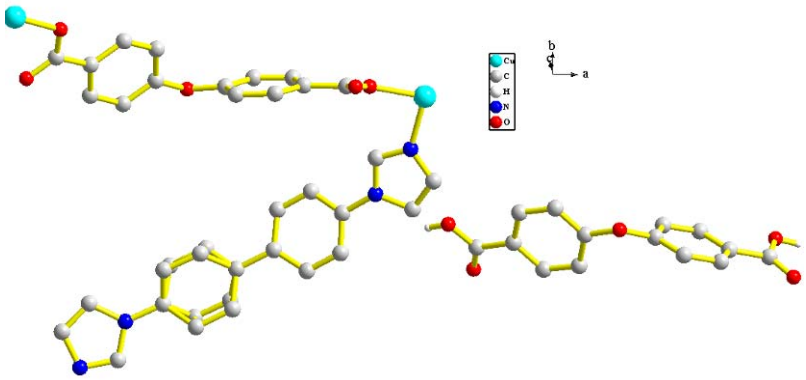

(a)

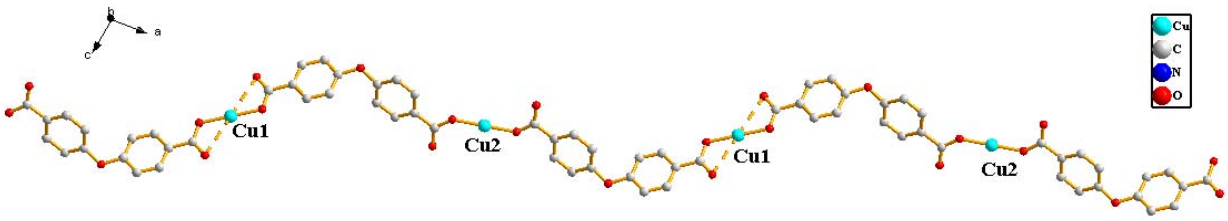

(b)

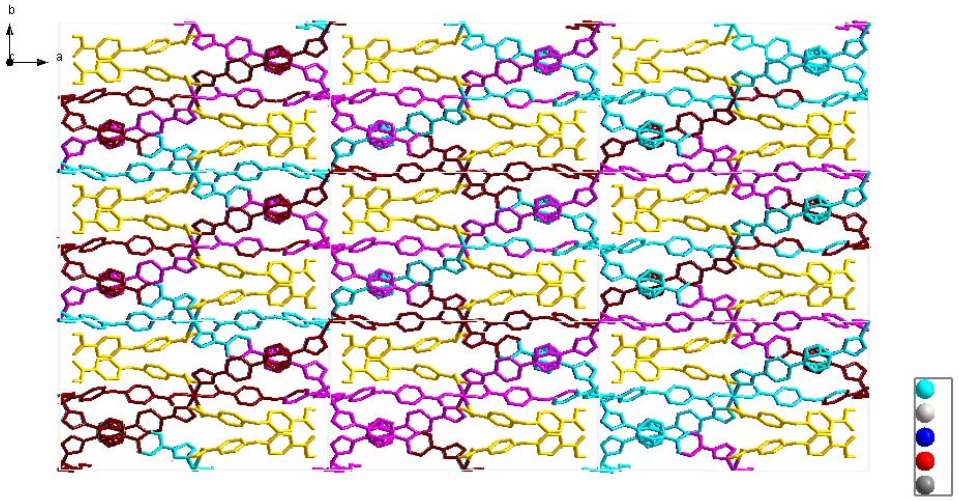

(c)

Fig. S1 (a) The asymmetric unit in **1**, (b) one-dimensional chain constructed from obba^{2-} and Cu^{2+}, (c) 3-fold parallel interpenetration of the 3D nets in **1**.

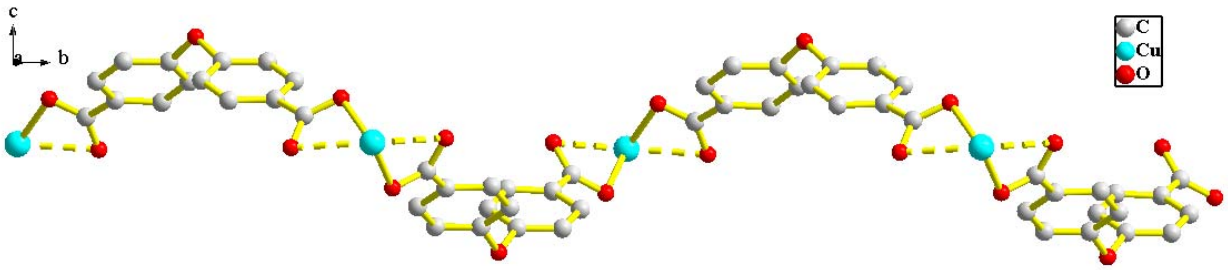

Fig. S2 The one-dimensional chain constructed from obba^{2-} and Cu^{2+} in **5**.

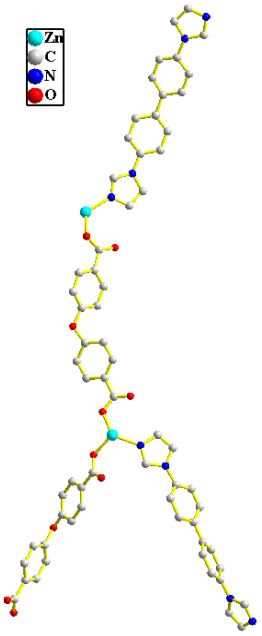

Fig. S3 The asymmetric unit in **6.**

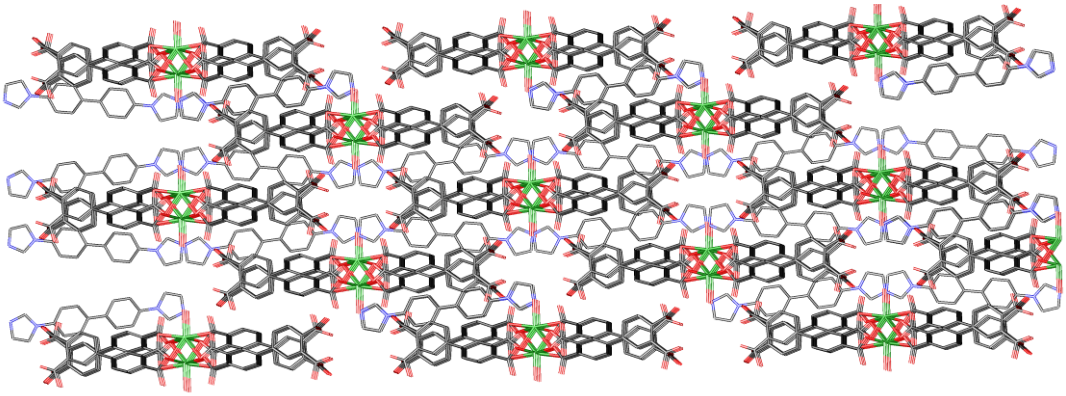

Fig. S4 The bimb moieties are located at an inversion center, which are included between the 1D chains in **6**.

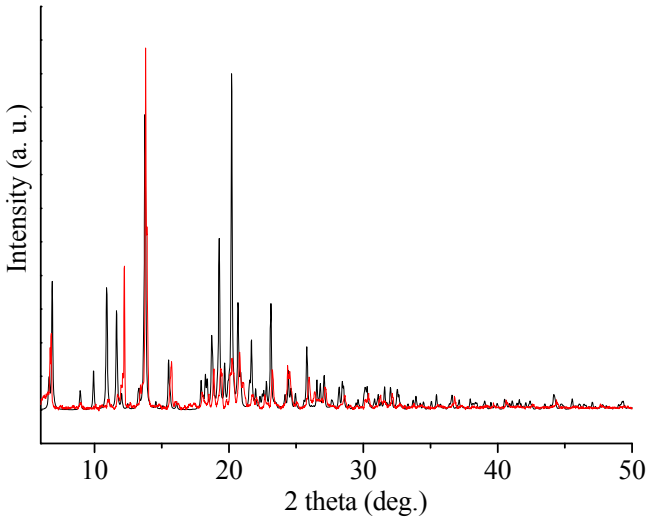

Fig. S5. X-ray power diffraction diagram of the simulated spectra from single crystal data of **1** (black) and compound **1** (red).

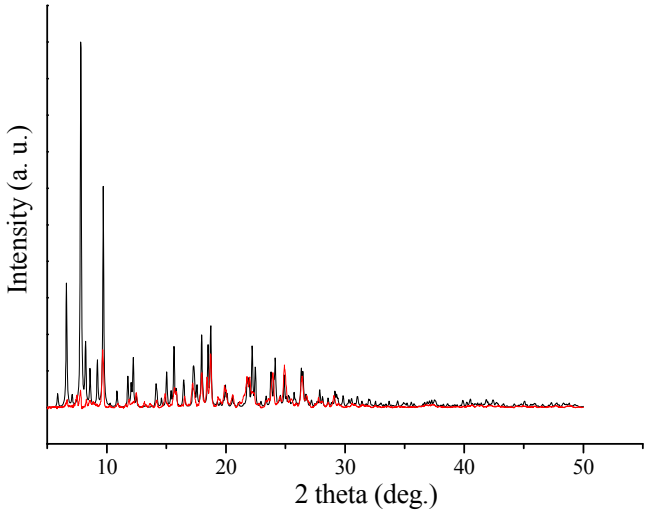

Fig. S6. X-ray power diffraction diagram of the simulated spectra from single crystal data of **2** (black) and compound **2** (red).

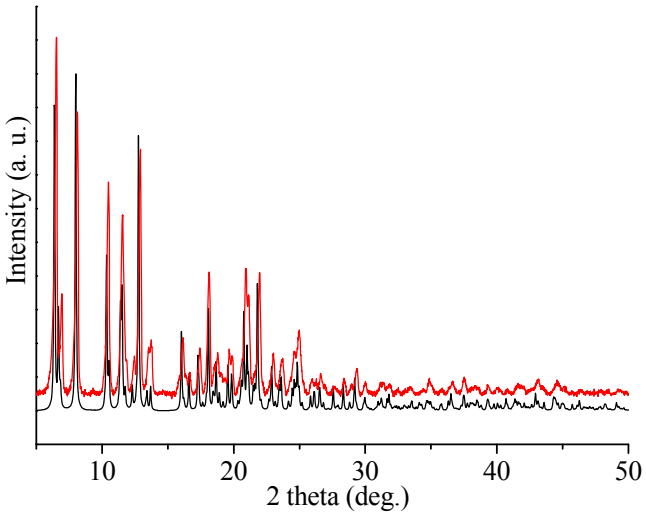

Fig. S7. X-ray power diffraction diagram of the simulated spectra from single crystal data of **3** (black) and compound **3** (red).

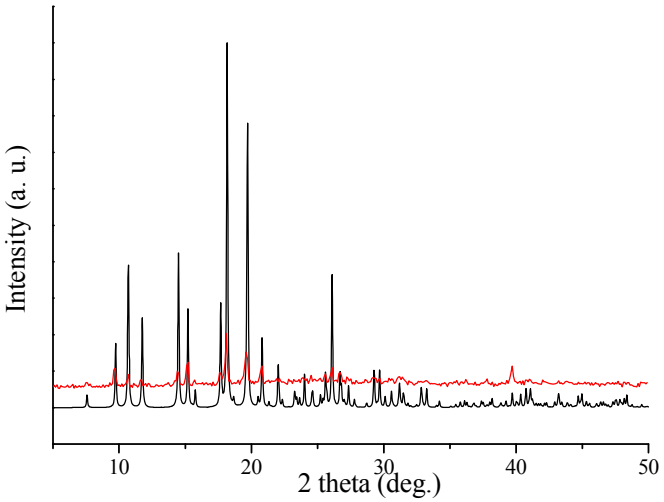

Fig. S8. X-ray power diffraction diagram of the simulated spectra from single crystal data of **4** (black) and compound **4** (red).

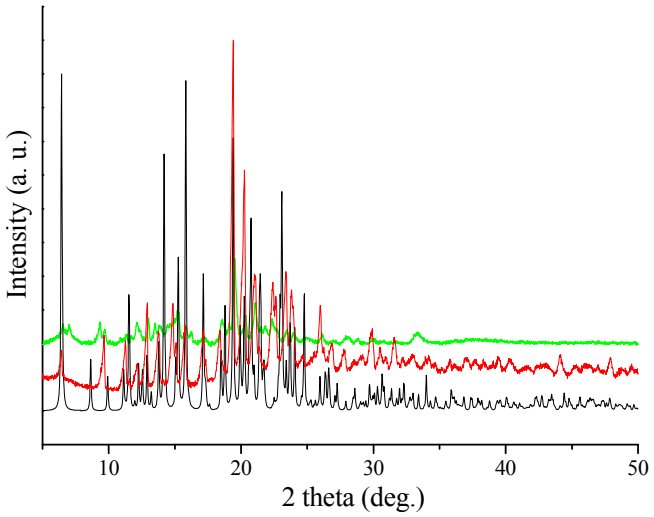

Fig. S9. X-ray power diffraction diagram of the simulated spectra from single crystal data of **5** (black), compound **5** (red), **5** after photocatalysis process (green).

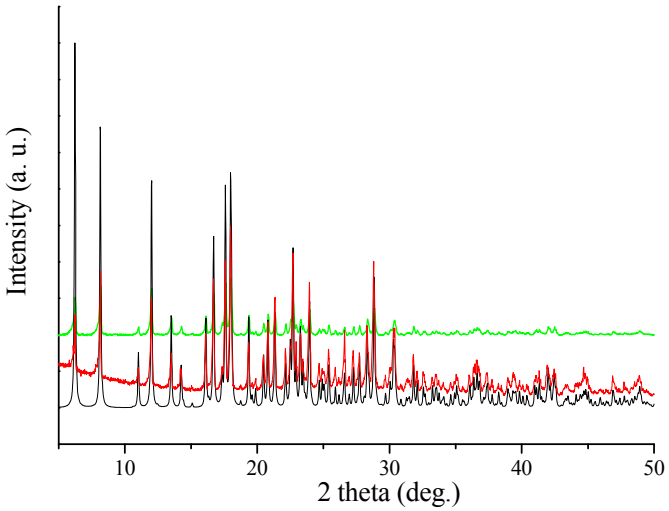

Fig. S10. X-ray power diffraction diagram of the simulated spectra from single crystal data of **6** (black), compound **6** (red), **6** after photocatalysis process (green).

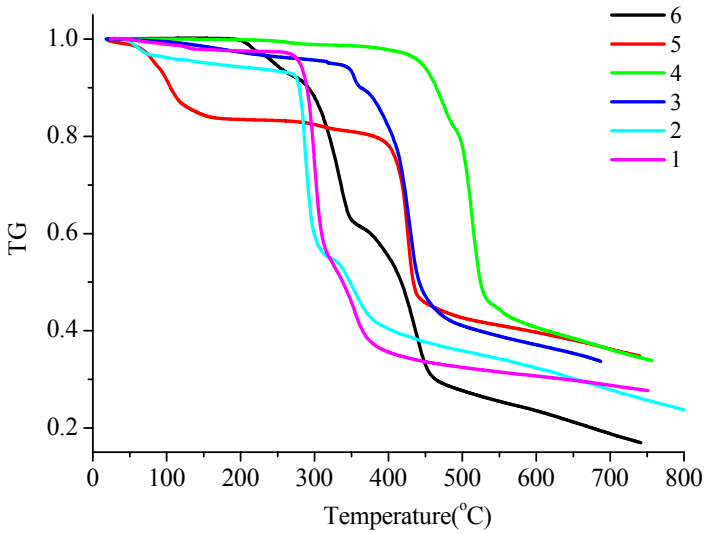

Fig. S11 TG curves of compounds **1-6.**

Both Compounds **1** and **2** are stable up to 265 °C where the organic groups start to decompose. Compounds **3** and **4** also have demonstrated high thermal stabilities, which are stable up to 344 and 410 °C, respectively, where the framework structures begin to collapse. For **5**, the weight loss of 17.10 % below 185 °C (calcd□ 17.73 %) corresponds to the loss of six coordinated aqua molecules, two free water molecules and two DMF guest moieties per formula. A plateau region is observed for **5** from 185 to 400 °C and consecutive decompositions suggest the total destruction of the framework. In addition, compound **6** is stable up to 200 °C.